Towards the realization of an optical pressure standard

Towards the realization of an optical pressure standard

D Mari[1], M Pisani[1] and M Zucco[1]

1. *Istituto Nazionale di Ricerca Metrologica (INRIM), Strada delle Cacce 91, 10135 Torino, Italy*

Email of corresponding author: d.mari@inrim.it

Abstract: A novel pressure standard based on optical interferometry has been realized. The paper presents a preliminary achievement of the developed system, in which the standard pressure between 1 kPa and 120 kPa is obtained through the measurement of the refractive index of a gas. The response of the optical system has been initially evaluated measuring its sensitivity for nitrogen and air, in terms of the ratio between a pressure variation and its consequent number of detected interferometric fringes. Afterwards, the interferometer has been geometrical characterized in order to perform an absolute measurement of the refractive index of the gas, allowing an optical measurement of the gas pressure. The following step has been to compare the results of a series of measurements by the optical system with a reference pressure standard at 120 kPa. Finally, the standard has been compared with two capacitance diaphragm gauges in the range between 1 kPa and 120 kPa.
The developed standard has a relative standard uncertainty equal to 170 ppm at atmospheric pressure.

Keywords: Pressure metrology; vacuum standard; laser interferometry; absolute distance; vacuum gauge, refractometry

1. Introduction

Pressure standards below 120 kPa are realized with different systems, depending on the pressure range. Standard pressures below 100 Pa are normally realized by primary standards based on static or dynamic expansion of pure gas [1-4]. The range between 100 Pa and 10 kPa is usually covered by pressure balances which work with a non-rotating piston-cylinder assembly and a balance as force meter [5, 6]. Above 10 kPa the standard pressure is obtained by traditional pressure balances [7] or mercury manometers [8]: these last have the advantage to be the only primary standards which are able to cover the whole pressure range between 100 Pa and 120 kPa. The history of mercury in pressure measurement is ancient and started in the XVII century, when Evangelista Torricelli realized the first vacuum experiment using mercury [9].
Over the centuries, the mercury manometers were improved until current sophisticated realizations aimed mainly to measure with high accuracy and precision the heights of mercury columns. Nevertheless such mercury-based system are not in line with recent Word Health Organization resolutions which recommend the progressive reduction of human exposure to mercury and mercury compounds.

The present paper describes a preliminary study of an optical realization of a pressure standard in the pressure range between 1 kPa and 120 kPa by interferometric technique.

2. Method and system

The proposed method is based on the measurement of the refractive index of a gas by means of a homodyne Michelson interferometer and it is alternative to the realizations which use Fabry-Pérot cavities [10]

The light source is a frequency stabilized He-Ne laser (wavelength $\lambda \approx 633$ nm), coupled to a polarization maintaining fiber ending with a collimator to launch the radiation in the interferometer.

In figure 1 the schematic of the heart of the apparatus is shown: a homodyne Michelson laser interferometer with fixed arms, in which the measurement arm consists essentially of a double mirror multiplication set-up, where the beam is reflected several times between two quasi-parallel mirrors A and B [11, 12], while in the reference arm the laser beam is sent to the mirror M_R.

The double mirror multiplication set-up allows to obtain a number *N* of reflections depending on the incidence angle on mirror A and the angle between mirrors A and B [11].

The reference and measurement beams are recombined by the beam splitter BS where interference occurs. After a passage through a polarizer P, the interference fringes, in the form of dark or bright pattern, are detected by the CMOS sensor of a high speed camera. The experiment is controlled by a software, which manages the acquisition and the analysis of data.

The interferometer is designed to be as stable as possible in temperature: the mirrors A and B are realized with Ultra Low Expansion ceramic glass (Clearceram®) and bonded to a circular plate made of the same material having nominal diameter 160 mm, with “hydroxide bonding” technique, practically behaving as a single glass block. The mirrors were bonded at an angle of about 0.4 ° and have nominal dimensions: width = 70 mm, height = 20 mm and thickness = 10 mm.

The plate is equipped with a circular aperture to facilitate the pumping process and placed on suitable kinematic spherical supports to reduce mechanical stresses and vibrations during gas inlet or pumping process. All remaining optical components of the interferometer are glued on the plate, which is inserted in a stainless steel pressure chamber V_1 of nominal internal diameter equal to 180 mm and height of 62.5 mm that is the chamber in which the standard pressure *p* is generated.

A detailed explanation of interferometer operation is reported in [12].

V_1 is connected to a pumping system by an exchangeable conductance, placed in a double-knife CF40 flange; a KF40 butterfly valve is placed between the pumping system and the conductance.

A barometer, calibrated against INRIM HG5 primary standard [8] and two capacitance diaphragm gauge (CDG 133 kPa full scale and 1.33 kPa full scale) are mounted on three ports of V_1

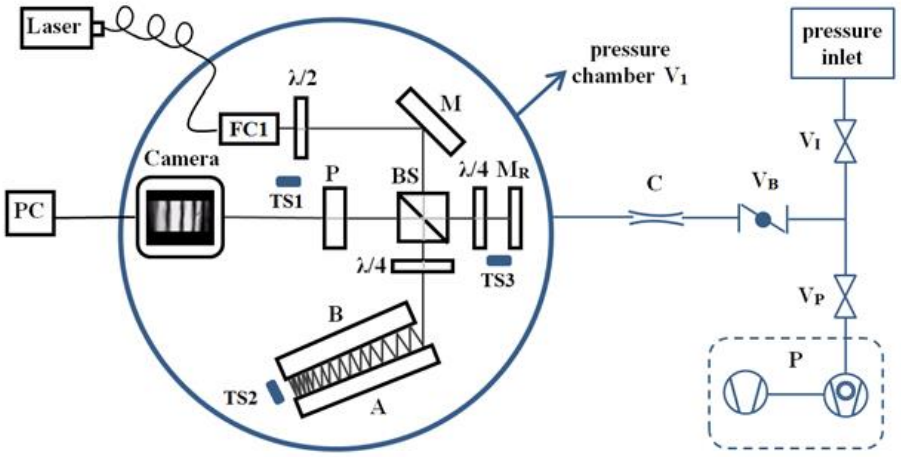

Figure 1. Schematic of the system with laser interferometer placed inside pressure chamber V_1; C: exchangeable conductance; TS: temperature sensors (PT100); V_B: butterfly valve; V_P: pump valve; V_I: inlet system valve; P: pumping system.

At the beginning of operation, V_1 is pumped at an ultimate pressure p_0 of the order of 0.1 Pa. The refraction index $n_{vac} \approx 1$ at p_0 is the reference condition of the optical system.

Subsequently, the standard pressure p_i is generated inside V_1, by inlet the gas inside the calibration chamber to reach the desired nominal value and after waiting a time sufficient for temperature stabilization. The absolute refractive index n_i associated to standard pressure p_i can be estimated by:

$$n_i = n_{vac} + \frac{\varphi_i \frac{\lambda}{2}}{L} \approx 1 + \frac{\varphi_i \frac{\lambda}{2}}{L} \quad (1)$$

where φ_i is the number of interference fringes occurred between the initial reference pressure p_0 and p_i, λ is the laser wavelength and L is the unbalance of the interferometer under vacuum, i.e. the optical path difference between reference and measurement arm of the interferometer, which was measured with the method described in chapter 3.1.

The Lorentz-Lorenz equation provides the link between the refractive index and the molar density ρ_i [13, 14]:

$$\rho_i = \frac{n_i^2 - 1}{n_i^2 + 2}\frac{1}{A} \tag{2}$$

where A is the molar refractivity [15].

Finally, neglecting the terms higher than the second order, the standard pressure p_i can be obtained by the equation:

$$p_i = \rho_i R T_i (1 + B_i \rho_i) \tag{3}$$

in which R is the universal gas constant, B_i the second order density virial coefficient [16, 17] *at temperature* T_i, which is the temperature inside V_1 at pressure point p_i. T_i is measured by a set of traceable temperature sensors, as showed in figure 1.

3. Experimental details and results

3.1 The measurement of the unbalance of the interferometer

The unbalance of the interferometer was measured by means of a dedicated experiment reported in figure 2 where a fiber coupled diode laser at 640 nm is amplitude-modulated at modulation frequency f_M, using a bias-T on the bias current, thus creating a synthetic wave with wavelength Λ:

$$\Lambda = \frac{v_g}{f_M} \tag{4}$$

where v_g is the group velocity of the synthetic wave at 640 nm.

The radiation from the laser is divided in two beams: one beam goes directly to the photodetector PD2 that generates the reference signal at f_{M2}, whereas the other beam is fed to the input port of the interferometer. The photodetector PD1 at the output port of the interferometer generates the measurement signal at f_{M1}. In general, from the phase difference between the two signals f_M from the two photodetectors it is possible to obtain the difference of the paths in term of the synthetic wavelength Λ. Since the measured phase contains information only regarding the excess fraction of wavelength, the ambiguity is resolved by changing

opportunely the value of the synthetic frequency f_M. In our case, on the photodetector PD1, we have the superposition of the beams coming from the two arms of the interferometer. In order to measure effectively the unbalance of the interferometer, i.e. the relative difference of the two arms, we measured alternatively the phase difference between the two signals (PD1 and PD2) blocking alternatively one of the two arms of the interferometer.

The resolution of the measurement decreases by increasing the modulation frequency f_M: with frequencies of some GHz, corresponding to synthetic wavelengths of some tens of mm, we can achieve a resolution of fractions of mm. The signals from PD1 and PD2 are then down-converted at the super-heterodyne frequency f_{sh}= 100 kHz by mixing them with a signal at f_R = f_M+100 kHz. The phase information of the signal at the GHz level is maintained in the down conversion to the super-heterodyne frequency at 100 kHz. The signals at 100 kHz are finally acquired by an acquisition board having two parallel DAQ and the phase difference is calculated with an algorithm based on I/Q demodulation.

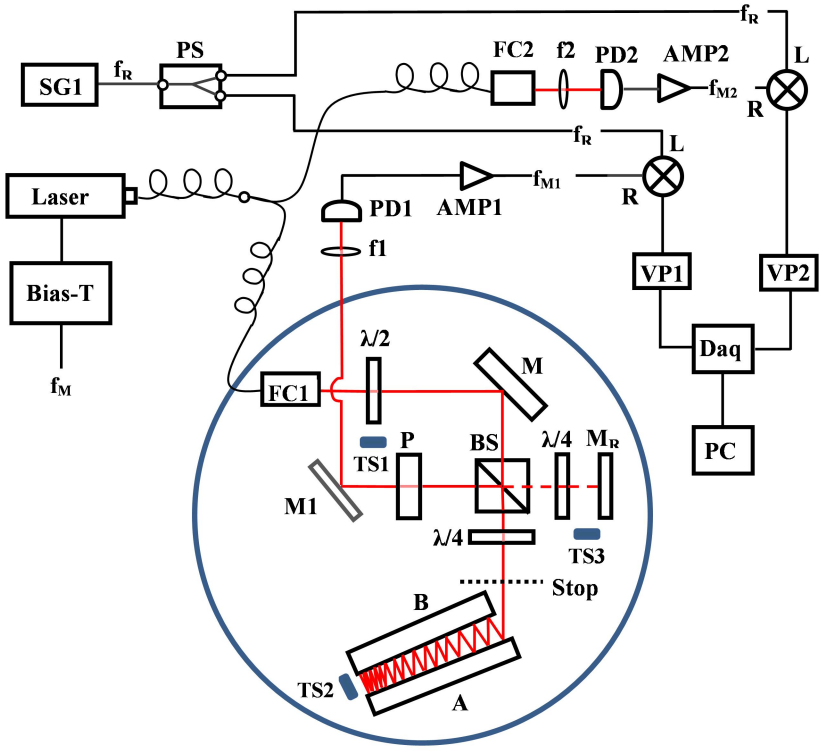

Figure 2. Schematic of the system for the absolute measurement of the difference between the two arms of the interferometer; M1: deflection mirror; SG: signal generators; PS: power splitter; FC: fiber coupler; f: lens; PD: photo-detector; AMP: amplifier; L, R: mixer channels; VP: voltage preamplifier.

The graph of the measured unbalance L for different synthetic frequencies ranging from 0.7 GHz to 1.3 GHz is reported in figure 3. Each point is the result of the difference between the path lengths switching alternately from one arm to the other with a time interval of the order of some minutes. The resulting unbalance length of the interferometer in vacuum is L= (1.4717 ± 0.0002) m, after having corrected for group velocity and where the main contribution to the uncertainty is due to repeatability, calculated as the standard deviation of the mean. Several normality tests have been performed to assess the use of the standard deviation of the mean to estimate the repeatability of the data presented in figure 3: as example, the p-value of Kolmogorov-Smirnov and Shapiro-Francia tests resulted greater than 0.90 for both tests, supporting the null hypothesis of normal distribution at 0.05 of significant level. The dispersion of the data could be caused by the non-complete cancellation of common mode effects due for example to the fiber length drifts during the minutes of measurements.

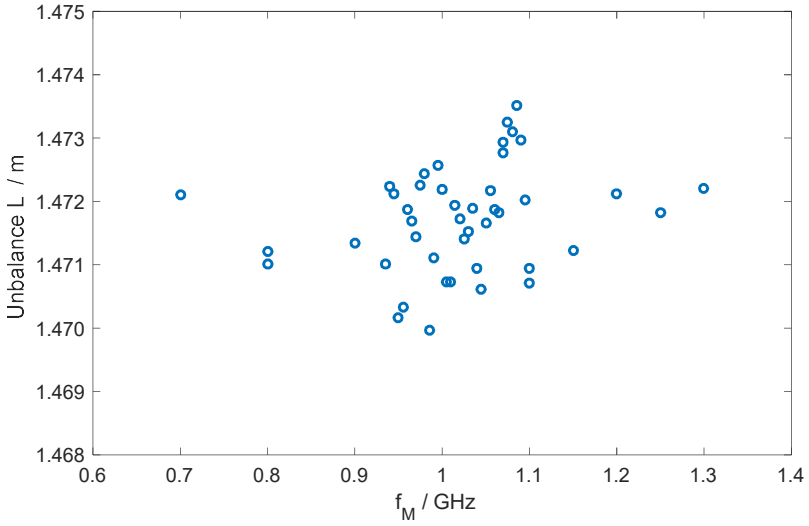

Figure 3. Unbalance L of the interferometer calculated for different f_M. Each point is the result of the difference of the two path length taking into account the separate interferometer arms.

3.2 Pressure measurement by optical technique

In the present chapter two possible approaches for pressure measurement by our optical system are described. The first, referred as the "sensitivity method" allowed to use the device as an optical pressure sensor, which needs to be periodically calibrated by a pressure reference standard. The second, named the "method of the absolute refractive index" allowed to consider the device as a pressure standard through the geometrical calibration of the interferometer arms.

3.2.1 Sensitivity method

The first step to evaluate the response of the optical system shown in figure 1, was the measurement of sensitivity S in terms of the ratio $\Delta p/\Phi \approx p_s/\Phi$ where Δp is the difference between pressure p_s (generally in the range between 120 kPa and 130 kPa) and base pressure p_0 and Φ is the total number of fringes detected during the pressure variation Δp; p_s is measured by a barometer, calibrated against INRIM primary standard HG5 [8]: its standard uncertainty is equal to 5 Pa in the considered pressure range.

The pressure change from p_0 to p_s was carried out by a slow inlet process of the gas in the pressure chamber V_1 in order to make negligible the initial temperature change occurred in case of fast pressure variation [18, 19] and minimize mechanical stress on the system occurred in case of fast pressure change; a variable leak valve was placed in series with the exchangeable conductance and regulated to obtain an inlet time of V1 of the order of 300 s. The measurement of S has been performed for 6 months after having aligned the interferometer to obtain an optimal setting in terms of number of reflections on the double mirror multiplication set-up, signal intensity and fringe contrast. The figure 4 shows the results of sensitivity values for nitrogen and ambient air, at standard temperature $T_{st} = 20$ °C.

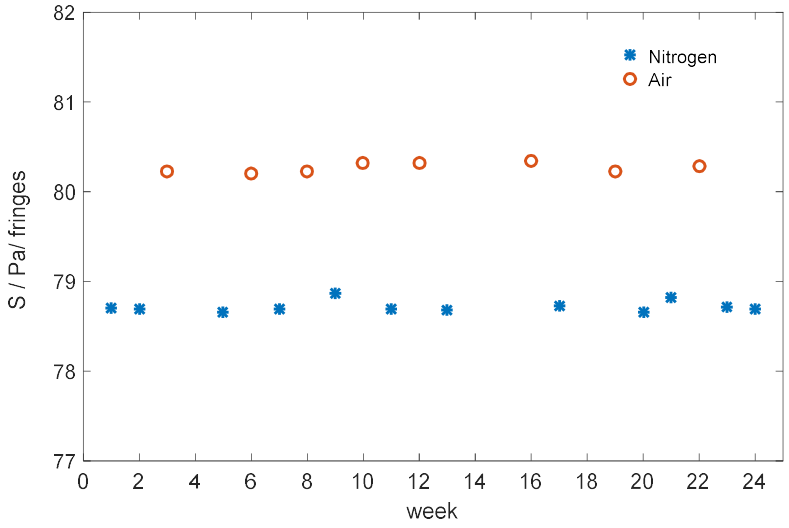

Figure 4. Sensitivity S (Pa/number of fringes) of the interferometer in a time interval of six months for air and nitrogen.

The sensitivity value and its standard uncertainty for nitrogen was found to be equal to (78.718±0.014) Pa/fringe, where the uncertainty was been evaluated taking into account also the long term stability of the pressure transducer; similarly for air, the value (80.322±0.030) Pa/fringe was obtained. The sensitivity results for nitrogen and air are in agreement with data of table 1 presented in [13].

At the end of this first stage study regarding the sensitivity, it is meant to emphasize that, as first results, the developed system could be used as pressure "sensor" (sensitivity method) using the proper normalized sensitivity of each gas S_{gas} at standard temperature T_{st} to obtain the pressure p_j simply measuring the correspondent number of fringes φ_j occurred between the initial reference pressure p_0 and p_j at the temperature T_j:

$$p_j = \varphi_j S_{gas} \frac{T_j}{T_{st}} \tag{5}$$

where the influence of temperature on φ_j through the thermal expansion of the Clearceram® can be considered negligible. As, during these months, the interferometer was maintained in the same condition without any optics realignments and the pressure transducer checked once a month, the obtained results also express the intrinsic long term stability of the whole apparatus, when it is used as sensor.

In this case, the measurement procedure requires an initial metrological characterization of the sensitivity S related to gases of interest, which has to be repeated whenever the interferometer needs to be realigned and a periodic measurement of S for each considered gases (typically once a year), to check if the new values are consistent with the previous one.

The uncertainty budget related to the "sensitivity method" is presented in chapter 4.

3.2.2 Method of the absolute refractive index

Afterwards, the second phase of the study described in the present paper was implemented to generate and measure standard pressure p_i following the method proposed in the chapter 2.

The essential pre-condition to operate rigorously according to this method, is the determination of unbalance L of the interferometer, which requires the dedicated experimental set up reported in the chapter 3.1. After the determination of unbalance L, in order to characterize the optical pressure standard, a series of measurement were performed in a period of about 6 weeks, at nominal pressure of 120 kPa following the measurement procedure described in the chapter 2:

1. pumping of the system to base pressure of the order of 0.1 Pa
2. gas (nitrogen) inlet to reach the nominal pressure p_i by a slow process
3. wait time for temperature stabilization (100 s)
4. measurement/acquisition of φ_i and T_i at pressure p_i and pressure p_b measured by the barometer
5. calculation of n_i by equation (1) and standard pressure p_i by equation (3), with the virial coefficient B_i obtained from [16, 17]

The results p_i were compared with the pressure reading p_b from the calibrated barometer (standard uncertainty equal to 5 Pa).

The following figure shows the results in terms of relative difference between pressure measured by the optical system and reading from the barometer. The uncertainty bars in the figure were evaluated as described in chapter 4.2 and correspond to 1.7×10^{-4} . The relative differences at 120 kPa, plotted in figure 5, are in the range between -7.0×10^{-5} and $+ 9.4 \times 10^{-5}$ (mean value: 1.3×10^{-5}) well below the evaluated relative standard uncertainty of 1.7×10^{-4}.

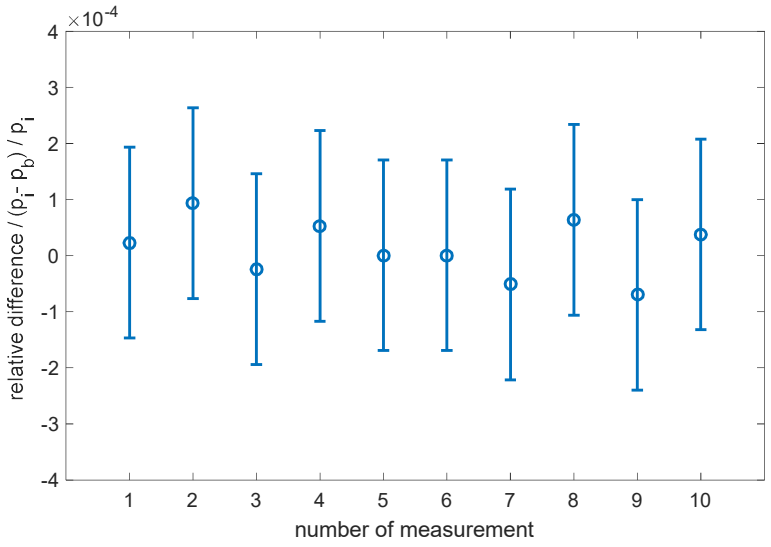

Figure 5. Relative difference $(p_i-p_b)\ /p_i$ at 120 kPa; p_i: measured by the optical system, p_b: reading from the barometer

Subsequently, a series of measurement cycles in a period of about 2 months were carried out to test the system, following the same procedure described previously with the pressure readings performed by a set of two CDGs to cover a pressure range between 1 kPa and 120 kPa for each measurement cycle. Each cycle was completed repeating the measurement procedure from point 2 to 5 for each pressure value.

The results are presented in the figure 6, where the relative difference between standard pressure p_i measured by optical system and the CDGs reading pressure $p_{i,CDG}$ is plotted as function of pressure.

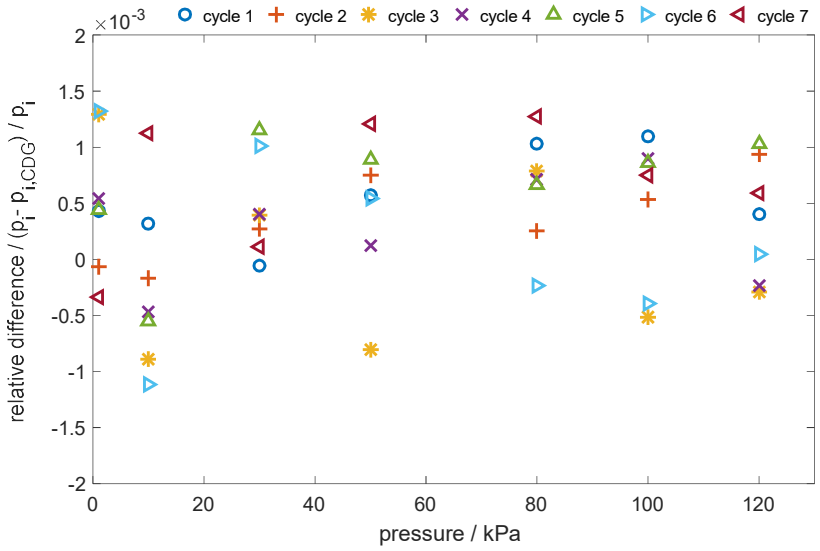

Figure 6. Relative difference $(p_{i,}\text{-}p_{i,CDG})\ /p_i$ as function of pressure The dispersion of the data is mainly due to the uncertainty of the pressure transducer used for the comparison.

The results obtained by optical system and the CDGs can be considered consistent, as the observed absolute relative differences are in accordance with relative standard uncertainty related to CDGs, equal to 2×10^{-3}. Furthermore, by comparing the results highlighted in figure 5 (carried out with a calibrated barometer with low uncertainty) with the results in figure 6 at 120 kPa, we deduced that the data dispersion shown in figure 6 was not due to the optical system, but to the different pressure transducers.

4. Uncertainty budget

4.1 Sensitivity method

The model equation for uncertainty evaluation in case of the "sensitivity method", as described in paragraph 3.2.1, is represented by eq. 5: the associated uncertainty budget is summarized in the table 1.

The sensitivity value and its uncertainty is calculated as described in paragraph 3.2.1.

The number of interference fringes φ_j occurred between the initial reference pressure p_0 under vacuum and the pressure p_j is determined by the method reported in [12]. The current standard uncertainty is 0.05 fringes.

The temperature T_j is measured by a set of PT100 sensors, calibrated in accordance with ITS90, by means of triple point of water and the melting point of gallium. The standard uncertainty is 0.029 K, taking into account calibration, repeatability and temperature gradients inside volume V_1.

Input x_j	Value	Source of uncertainty	$u(x_j)$	$c_i\, u(x_j)/\, p_j$	% Variance
S	78.718 Pa /fringes	Sensitivity determination: calibration uncertainty, repeatability, stability	0.014 Pa /fringes	1.82×10^{-4}	74.6 %
φ_j	1271.76 fringes	Repeatability, systematic effects	0.05 fringes	3.93×10^{-5}	3.5 %
T_j	293.342 K	Calibration uncertainty, repeatability, temperature gradients in chamber V_1	0.029 K	9.88×10^{-5}	21.9 %
$u_c(p_j)/\, p_j$		(combined relative standard uncertainty)		2.1×10^{-4}	100%

Table. 1. Example of uncertainty budget for nitrogen at p_j=100176 Pa (sensitivity method). The percentage in the last column is the relative contribution of each variance to the total variance.

The previous table shows clearly that the combined standard uncertainty depends dramatically on the component due to gas sensitivity determination, nevertheless, as first approach, the "sensitivity method" allows to cover the pressure range between 1 kPa and 120 kPa by means of a single measuring system with a relative standard uncertainty of 2.1×10^{-4} at atmospheric pressure.

4.2 Method of the absolute refractive index

The model equation for uncertainty evaluation of the "method of the absolute refractive index" can be derived from equations (1-3) and it is given by:

$$p_i = \frac{\left(1+\frac{\varphi_i \frac{\lambda}{2}}{L}\right)^2 - 1}{\left(1+\frac{\varphi_i \frac{\lambda}{2}}{L}\right)^2 + 2} \frac{RT_i}{A} \left(1 + B_i \frac{\left(1+\frac{\varphi_i \frac{\lambda}{2}}{L}\right)^2 - 1}{\left(1+\frac{\varphi_i \frac{\lambda}{2}}{L}\right)^2 + 2} \frac{1}{A} \right) \tag{6}$$

The measurement of temperature T_i and the evaluation of its uncertainty have been obtained as described in the previous paragraph.

The molar refractivity A for nitrogen adopted in the present work is derived from [15]: its standard uncertainty is equal to 0.6×10^{-10} m^3/mol.

The number of interference fringes φ_i measured between the initial reference pressure p_{ref} and standard pressure p_i is determined by the method reported in [12], with standard uncertainty of 0.05 fringes.

The laser source is a commercial stabilized He-Ne laser; the standard uncertainty of its wavelength is 9.5×10^{-13} m evaluated according to CIPM recommendation, as described in [20].

The values of the unbalance of the interferometer L and its standard uncertainty were determined following the method described in the paragraph 3.1. The standard uncertainty is equal to 0.0002 m.

The second order density virial coefficient B_i and its uncertainty were determined according to [16, 17] with standard uncertainty of 2.4×10^{-7} m^3/mol

The uncertainty budget related to the model equation (5) at p_i=100164 Pa is summarized in the table 2

Input x_i	**Value**	**Source of uncertainty**	**$u(x_i)$**	**$c_i\, u(x_i)/\, p_i$**	***% Variance***
T_i	293.124 K	Calibration uncertainty, repeatability, resolution, temperature gradients in chamber V_1,	0.029 K	9.89×10^{-5}	32.5 %
A	4.44585×10^{-6} m3/mol	Molar refractivity [15]	6×10^{-11} m^3/mol	-1.35×10^{-5}	0.6 %
φ_j	1274.82 fringes	Repeatability, systematic effects	0.05 fringes	3.92×10^{-5}	5.1 %
λ	632.9908×10^{-9} m	Laser wavelength [18]	9.5×10^{-13} m	1.50×10^{-6}	0.0 %
L	1.4717 m	Calibration uncertainty, resolution, repeatability, stability	0.0002 m	-1.36×10^{-4}	61.5 %
B_i	-5.95×10^{-6} m^3/mol	[16, 17]	2.4×10^{-7} m^3/mol	9.87×10^{-6}	0.3 %
$u_c(p_i)/\, p_i$		(combined relative standard uncertainty)		1.7×10^{-4}	100%

Table 2. Example of uncertainty budget at p_i=100164 Pa, nitrogen. The percentage in the last column is the relative contribution of each variance to the total variance.

The realized pressure standard has a relative standard uncertainty of 170 ppm at atmospheric pressure: this result has to be intended as the first preliminary step towards an optical realization of the Pascal. The future developments of the present work aim to revise the whole experimental set-up as well as the measurement procedure to obtain a pressure standard with a relative standard uncertainty of 5 ppm at atmospheric pressure. The main improvements needed to reach the target uncertainty of 5 ppm can be easily deduced from the table 2: in the current

experimental set-up, the main component of uncertainty of the combined standard uncertainty $u_c(p_i)$ are due to the measurement of the unbalanced L of the interferometer and to the temperature measurement inside the calibration volume V_1 .

The accurate measurement of temperature could result the most difficult challenge as requires further studies to change the current system layout and design a temperature control and measurement set-up able to obtain an uncertainty of the order of 0.3 mK, taking into account also the non-uniformity of temperature field inside V_1.

The measurement of the unbalanced L of the interferometer could be carried out with a different approach [21] to measure L with an associated uncertainty of about 3 μm: also this target will require changes in the optical set-up to improve the mechanical and thermal stability of the various components.

For what concern the measurement of fringes φ_i, it will be necessary improve the signal to noise ratio and reduce the effects of non-linearities of the interferometer as well as an implementation of a more complex compensation algorithm [22]. After that, helium could be used, because its refraction index can be obtained by first principles with high accuracy and its molar refractivity may be determined with lower uncertainty [23, 24, 25]; this fact would allow to compare the results obtained by "first principles calculations" with the measurement performed by the optical pressure standard to estimate the pressure dependence of thermo-mechanical deformations of the double mirror multiplication set- up.

At last, the mathematical model summarized in eq. 5 has to be modified to take into account the non-ideality of gas, introducing higher terms of density virial coefficients and refractivity virial coefficients in equations (2, 3) as reported in [13, 16, 26].

A new optical set-up and a new measurement procedure are under study to meet the requirements mentioned in the previous lines to achieve the goal of an optical realization of a pressure standard with an uncertainty of 5 ppm at atmospheric pressure.

5. Conclusions

The realization of a pressure standard via optical method has been presented. The system is able to work in the range between 1 kPa and 120 kPa and is based on the measurement of the refractive index of a gas by means of a multi-reflection homodyne interferometer.

The sensitivity of the optical system, in terms of the ratio between pressure and number of interference fringes, was measured for nitrogen and air, allowing as first approach, the use of the realized system as optical pressure sensor.

Subsequently, the absolute measurement of the unbalance L of the interferometer was carried out by an independent method based on the synthetic wavelength technique in conjunction with super-heterodyne detection.

The absolute determination of unbalance L made possible to use the system as absolute refractometer to realize a pressure standard: a series of measurements were performed at nominal pressure of 120 kPa and the results were consistent with the pressure reading from a calibrated barometer.

To complete the characterization of the new standard, the pressure determined by the optical method was compared to the pressure measured by a set of two reference transfer standards, obtaining results that are consistent with their uncertainty.

The uncertainty budget has evidenced that the realized pressure standard has currently a relative standard uncertainty of 170 ppm at atmospheric pressure: the achieved result has to be intended as first preliminary step towards a pressure standard via optical method, alternative to the realizations that use Febry-Pérot cavities and which could replace the mercury based current systems.

A new optical set-up and a new measurement procedure are under study, to obtain a pressure standard in the range between 100 Pa and 150 kPa, with a target relative standard uncertainty of 5 ppm at atmospheric pressure. In particular, the uncertainty associated to the gas temperature and the interferometer unbalance length will be reduced. The first one by adopting an active thermal stabilization system and the second by using a more complex technique for the absolute length measurement of the unbalance of the interferometer.

Aknowledgement

The authors are grateful to D. Corona (INRIM) for the useful discussions and the calibration of the temperature sensors, L. Iacomini and F. Bertiglia (INRIM) for their support in the temperature measurement system.

The authors also wish to thank P. Cordiale, E. Audrito and S. Pasqualin (INRIM) for their essential help during the realization of the measurement system described in the present paper.

References

[1] Jitschin W 2002 *Metrologia* **39** 249-61.

[2] Bergoglio M and Calcatelli A 2004 *Metrologia* **41** 278-84.

[3] Jousten K, Menzer H, Wandrey D and Niepraschk R 1999 *Metrologia* **36** 493-497.

[4] Bergoglio M, Mari D 2009 *Vacuum* **84** 270-73.

[5] Rendle C G and Rosenberg H 1999 *Metrologia* **36** 613-16.

[6] Ooiwa A 1994 *Metrologia* **30** 607-10.

[7] Sutton C M and Fitzgerald M P 2009 *Metrologia* **46** 655-60.

[8] Alasia F, Birello G, Capelli A, Cignolo G and Sardi M 1999 *Metrologia* **36** 499-503.

[9] Middleton W E K 1964 *The history of the barometer* (Baltimore: John Hopkins University Press).

[10] Egan P F, Stone J A, Hendricks J H, Ricker J E, Scace G E, Strouse G F 2015 *Optics Letters* **40** 3945-48.

[11] Marco Pisani 2009 *Meas. Sci. Technol.* **20** 084008.

[12] Mari D, Bergoglio M, Pisani M and Zucco M 2014 *Meas. Sci. Technol.* **25** 125303.

[13] Pendrill L R 2004 *Metrologia* **41** 40-51.

[14] Pendrill L R 1988 *Metrologia* **25** 87-93.

[15] Egan P and Stone J A 50 2011 *Applied Optics*, **19** 3076-86.

[16] Dymond J D, Marsh K N, Wilhoit R C and Wong K C 2002 *Virial Coefficient of Pure Gases and Mixtures*, Landolt-Börnstein, Group IV: Physical Chemistry Vol. 21 (Berlin: Springer-Verlag).

[17] Egan P F, Stone J A, Ricker J E, and Hendricks J H, 2016 Review of Scientific Instruments **87,** 053113.

[18] Jousten K, Pantazis S, Buthig J, Model R, Wüest M and Iwicki J 2014 *Vacuum* **100** 14-17.

[19] Jousten K 1994 *Vacuum* **45** 1205-08.

[20] Stone J A, Decker J E, Gill P, Juncar P, Lewis A, Rovera G D and Viliesid M 2009 *Metrologia* **46** 11-18.

[21] van den Berg S A, van Eldik S and Bhattacharya N 2015 *Nature Scientific Reports* **5** 14661.

[22] Gregorčič P, Požar T and Možina J 2009 *Optics Express* **17** 16322-31.

[23] Stone J A and Stejskal A 2004 *Metrologia* **41** 189-97.

[24] Schmidt J W Gavioso R M May E F and Moldover M R 2007 *Physical Review Letters* **98** 254504.

[25] Moldover M R, Gavioso R M, Mehl J B, Pitre L, de Podesta M and Zhang J T 2014 *Metrologia* **51** R1-19.

[26] Achtermann H J, Magnus G and Bose T K 1991 *The Journal of Chemical Physics* **94** 8.